The influence of resistant force equations and coupling system on long train dynamics simulations

The influence of resistant force equations and coupling system on LTD simulations

Authors: N. Bosso[a], M. Magelli[a], L. Rossi Bartoli[a], N. Zampieri[a*]

a) Politecnico di Torino, Department of Mechanical and Aerospace Engineering, C.so Duca degli Abruzzi 24, 10129, Torino
*corresponding author: Nicolò Zampieri, e-mail: nicolo.zampieri@polito.it, Tel.: +390110906997, Fax.: +390110906999

Acknowledgments

The authors wish to thank Dr. Qing Wu, from Central Queensland University, for providing useful data about the wagons and locomotives considered in the benchmark simulation scenarios. The authors also wish to thank Professor Luciano Cantone, from Università degli Studi di Roma Tor Vergata, for providing the mechanical impedance characteristic of the European buffers and hooks.

Abstract

In the simulation of the longitudinal dynamics of long trains, the modeling of the resistant forces and of the coupling system are two essential aspects. The modeling of the resistant forces directly affects the speed reached by each vehicle as well as the in-train forces. A literature review witnesses different laws for the calculation of both ordinary and accidental resistances. One of the objectives of this paper is to evaluate from the numerical point of view the influence of the resistant forces modeling strategy on the simulation outputs, i.e., on the speeds and in-train forces, by comparing different laws for propulsion and curving resistances. For what concerns the connection between the vehicles of the train, it is well known that the connection system is of utmost importance for the safety and running stability of the train. In this paper, the two existing coupling systems, i.e., the European buffer-hook system and the coupler used outside the European continent are first described, both in terms of operation and modelling techniques, and then they are compared on the same simulation scenario. All the simulations are performed on the first scenario of the International benchmark of the longitudinal train dynamic simulators, using the LTDPoliTO code developed by the railway research team from Politecnico di Torino.

1. Introduction

The study of the longitudinal train dynamics (LTD) of long freight trains is of utmost importance to predict the speeds reached by the train and the in-train forces. The increase in the length of freight trains in recent years, in fact, has generated an increase in the in-train forces[1], which can lead to disastrous consequences such as the breakage of the coupling elements or the derailment of the train caused by excessive tensile and compressive forces, respectively.[2-4] LTD is strongly affected by the type of coupling element adopted for vehicle connections. Two main solutions exist nowadays, namely the buffer-hook system, installed on European vehicles, and the automatic coupler, used in the rest of the world, both sketched in Figure 1.[5]

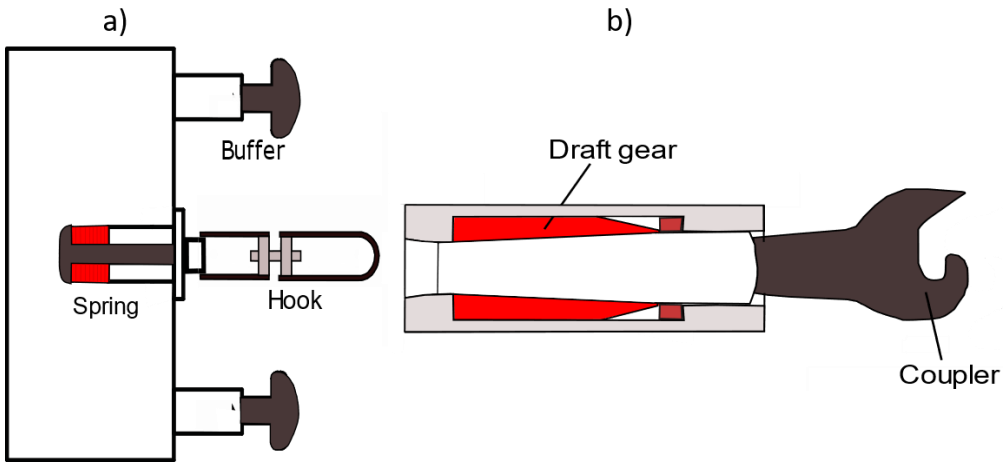

Figure 1: a) Schematic of the buffer-hook coupling system. b) Schematic of the coupler system.

The European system is completely manual and consists of two buffers, transmitting compressive loads, and a hook in series with a tensioner and an elastic group providing friction damping, that transmits tensile forces.[6, 7] On the other hand, the coupler is an automatic system consisting of two hooks which connect automatically when two adjacent vehicles approach to each other and it can transmit both tensile and compressive forces,

while the friction damping action is given by an elastic group named draft gear. Despite the advantages of the coupler over the buffer-hook system in terms of safety and maximum permissible loads, the coupler has not yet been adopted in Europe mainly for economic reasons, since the connection systems of thousands of vehicles circulating on the continent should be modified.

From the modelling point of view, the train system can be simulated considering only the longitudinal degree of freedom, treating the vehicles as concentrated masses connected to each other through non-linear elements that represent the coupling systems. This approach was also adopted in the recently established International benchmark of LTD simulators ("the benchmark" in the rest of the paper).[8, 9] The forces acting on the generic vehicle in the train composition are the resisting forces F_r, the traction and dynamic braking (DB) forces $F_{db/t}$ (equal to 0 if the vehicle is not a locomotive), the braking force of the pneumatic system F_{pb} and the in-train forces F_{ce}, as shown in Figure2, where x, $\dot{x}$, $\ddot{x}$ are respectively the position, the velocity and the acceleration of the vehicle. By applying the balance of forces to each vehicle, see Equation 1, where M_v is the total mass of the vehicle, we obtain a system of N non-linear ordinary differential equations, with N total number of vehicles.[10, 11]

$$M_v\ddot{x} = F_{db/t} + F_{ce,i/i+1} - F_r - F_{pb} - F_{ce,i/i-1} \quad (1)$$

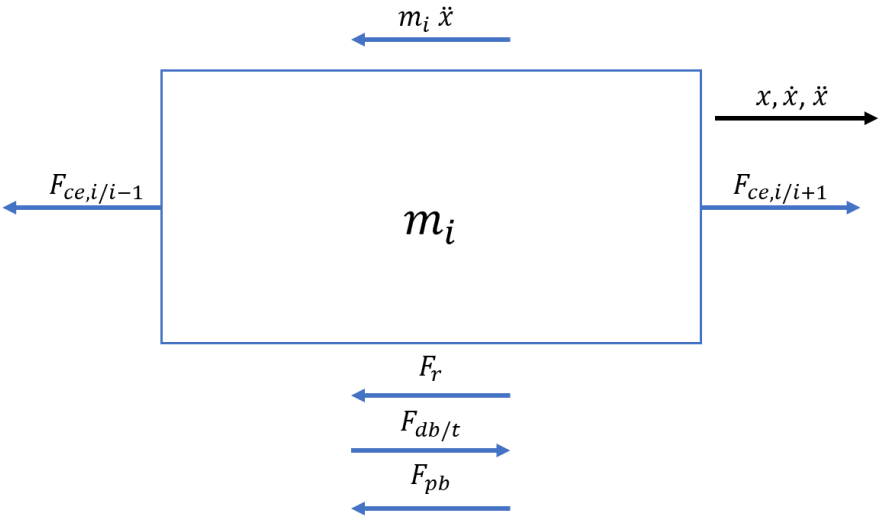

Figure 2: a) Free body diagram of a generic vehicle in the train composition.

The outputs computed by an LTD simulator thus depend on the modelling strategy adopted for the calculation of the in-train forces and on the expressions for the determination of the resistant forces.

The modeling of the coupling systems represents one of the most complex tasks in the simulation of longitudinal dynamics as it involves several nonlinearities to be considered, such as friction, slack, preload and the typical hysteresis cycle which is experimentally obtained in drop-hammer[12] tests.[13-15] The main techniques used to model these systems are three: i) look-up table (LUT) approaches[16-22], ii) mathematical functions fitting experimental data[23-32] and white-box models based on the physical and geometrical parameters of the system.[33-36]

Focusing on the resistant forces, they can be classified as ordinary or accidental forces. The first ones are present in the uniform and straight motion of the train and include the mechanical resistance due to rolling and friction between wheel and rail and the aerodynamic resistance. Accidental resistances, on the other hand, include the curving resistance and the resistance due to the slope of the track.

Ordinary resistances, also known as “propulsion resistances”, are usually modeled with a second order polynomial expression as a function of the vehicle speed V, see Equation 2, where the first two terms refer to the mechanical resistance component, while the last one to the aerodynamic component.[33, 37, 38] Several laws are witnessed in the literature with polynomial coefficients depending on the type of considered vehicle, as noticeable in Table 1, where r indicates the specific resistance expressed in N/tonne, m_a the axle-load in tons, n the number of axles and V the vehicle speed in km/h. [33, 39, 40]

$$F_{R,ord} = A + BV + CV^2 \tag{2}$$

Table 1: List of propulsion specific resistance laws for wagons.

	Wagons
Benchmark	$r = \left(2.943 + \frac{89.2}{m_a} + 0.0306V + \frac{0.122V^2}{m_a n}\right)$
Original Davis	$r = 6.376 + \frac{129}{m_a} + BV + \frac{CV^2}{m_a n}$
Modified Davis	$r = 2.943 + \frac{89}{m_a} + 0.0305V + \frac{1.718 k_{ad} V^2}{m_a n}$
Eig Ton France	$r = 9.81 \cdot \left(1.2 + \frac{V^2}{4000}\right)$
Heavy Freigth France	$r = 9.81 \cdot \left(1 + \frac{V^2}{4000}\right)$
German Strahl Full	$r = 10 \cdot \left(c_0 + (0.007 + c_1) \cdot \left(\frac{V}{10}\right)^2\right)$ $c_0 = 1.4\ full\ wagons$ $c_0 = 2\ empty\ wagons$ $c_1 = 0.025\ for\ 4 - axle\ wagons$
China Full Freigth	$9.81 \cdot (0.92 + 0.0048V + 0.000126V^2)$
Australia Min. Full	$5.17 + 0.010997V + 0.00051V^2$
Full Freigth CZE	$9.81 \cdot (1.3 + 0.00015V^2)$
Russian	$9.81 \cdot \left(0.7 + \frac{3 + 0.1V + 0.0025V^2}{m_a}\right)$
DeutchBahn Full Freigth	$9.81 \cdot \left(1 + 0.1 \cdot 0.2 \cdot \left(\frac{V}{10}\right)^2\right)$
Serbian Formula	$9.81 \cdot (4.83 \cdot 10^{-1} + 1.83 \cdot 10^{-2}V + 1 \cdot 10^{-4}V^2)$
Koffman BR carriages	$9.81 \cdot (1.1 + 0.021V + 0.000175V^2)$
	Locomotives
Benchmark	$r = 3.2 \cdot \left(2.943 + \frac{89.2}{m_a} + 0.0306V + \frac{0.122V^2}{m_a n}\right)$
China SS4DC Loco	$r = 9.81 \cdot (2.25 + 0.019V + 0.00032V^2)$

China DF Diesel Loco	$r = 9.81 \cdot (2.93 + 0.0073V + 0.000271V^2)$
China HXD1 Loco	$r = 9.81 \cdot (1.4 + 0.0038V + 0.0003V^2)$
China HXD2 Loco	$r = 9.81 \cdot (0.84 + 0.0012V + 0.000313V^2)$
British Loco	$r = 9.81 \cdot (4.587 + 0.0245V + 0.00036697V^2)$

As regards the accidental resistances, the literature review[37, 41-43] highlighted three main expressions used for the calculation of the curving resistance, namely i) the benchmark law, suggested in the international benchmark, see Equation 3, ii) the Roeckl formula, see Equation 4, and iii) an equation depending on the wheelbase, see Equation 5, which is referred to as the wheelbase formula in the rest of the paper. Please note that in Equations 3-5, r_c indicates the specific curving resistance in N/tonne, a the wheelbase in meters and R_c is the curve radius in meter.

$$r_c = \frac{6116}{R_c} \tag{3}$$

$$r_c = \begin{cases} \dfrac{6500}{R_c - 55} & R_c > 350m \\ \dfrac{5300}{R_c - 35} & 250m < R_c < 350m \\ \dfrac{5000}{R_c - 30} & R_c < 250m \end{cases} \tag{4}$$

$$r_c = \frac{1600a + 1620}{R_c} \tag{5}$$

The resistance due to the track grade instead is usually modeled simply considering the component of the weight force parallel to the ground, according to Equation 6, where M_v is the total vehicle mass in kg, g is the gravitational acceleration and i_s is the track slope in ‰, therefore different LTD simulators tend to compute the same values of force.

$$F_g = \frac{M_v g i_s}{1000} \tag{6}$$

The aim of the present paper is the investigation of the outputs computed in LTD simulations using different laws for the calculation of the ordinary and curving resistant forces. In fact, since the railway literature witnesses many different expressions for the calculation of these forces, it is of paramount importance to verify whether different equations can lead to significant changes in the outputs computed by LTD simulators. Moreover, simulations are also carried out in the same simulation scenario considering long train with high axle-load wagons, using both the automatic coupler and the buffer-hook system as coupling elements, to investigate whether the development of new longer freight trains in Europe can still rely on the traditional system.

For the simulations, input data from the international benchmark of LTD simulators was used for the track data, the train configuration, the wagon connection systems and the locomotive traction and DB characteristics. Among the four trains proposed in the benchmark, only the first one was considered in this work because it requires the lowest computational effort since it has a lower number of vehicles, and because it is the most similar to European trains at least in terms of configuration, even though the wagon axle-load is above the European limits. It is therefore the only benchmark train configuration that can be used to perform the comparison between the European buffer-hook connection system and the automatic coupler used in the rest of the world.

The paper is organized as follows. In the following section, the LTD code LTDPoliTO, developed by the Politecnico di Torino railway research group and used to perform the simulations, is briefly described. Then, a subsequent section focuses on the description of the simulation scenario and on the simulations performed. Finally, the results obtained are

presented and discussed, and a last section deals with the conclusions of the numerical activity presented in this paper.

2. Description of the LTDPoliTO code

In this section, the LTDPoliTO code is briefly described. The code only considers the longitudinal degree of freedom, as usual in the simulation of the longitudinal dynamics of long trains, modeling the elevation and curvature of the track as extra resistant forces applied to each vehicle in the train. The wheel-rail contact is neglected as common to most LTD simulators since the calculation of the wheel-rail contact forces can be computationally expensive even in case fast algorithms[44-48] are used.

The pneumatic braking is not considered in accordance with the benchmark input, but the code will be updated in the future in order to include a pneumatic module for the simulation of the braking forces due to the air brake system.

The code was validated in previous works[49-51] on the four simulation scenarios proposed in the international benchmark of LTD simulators using the laws suggested by the benchmark for the computation of the resistant forces, see Table 1 and Equations 3 and 6. The code validation showed that the outputs computed by the new code are in good agreement with the other simulators joining the benchmark. Moreover, the code proved to be able to produce numerically stable results with good computational efficiency in all four train configurations. This was a big upgrade with respect to a previous LTD code developed by the authors[52, 53] using the Simpack multibody software package, which showed numerical instabilities and lower computational speeds.

The new code was upgraded in order to introduce the possibility of modifying the expressions for the calculation of the retarding forces, to perform the comparison among different resistant laws in terms of the simulation outputs, which is one of the main objectives of this work.

The in-train forces on the coupling systems are calculated with a LUT strategy as a function of the deflection Δx and relative speed Δv on each coupling element using for the coupler the mechanical characteristic provided by the benchmark. A linear smoothing approach, based on the work by Zhang et al.[3], is used to manage the transition between the loading and unloading curves, which occurs when the absolute value of the relative speed Δv is less than a threshold term v_ε. On the other hand, if the absolute value of the relative speed is greater than the threshold v_ε the loading or unloading force is applied, as stated by Equations 7-9.

$$F_C(\Delta x, t) = \begin{cases} F_{CM}(\Delta x, t) + F_{CA,j}(\Delta x, t)\,\mathrm{sign}(\Delta x \cdot \Delta v)\,, & |\Delta v| \geq v_\varepsilon \\ F_{CM}(\Delta x, t) + \dfrac{|F_{CA}(\Delta x, t)|}{v_\varepsilon}\Delta v, & |\Delta v| < v_\varepsilon \end{cases} \tag{7}$$

$$F_{CM}(\Delta x, t) = \frac{F_{CL,j}(\Delta x, t) + F_{CU}(\Delta x, t)}{2} \tag{8}$$

$$F_{CA}(\Delta x, t) = \frac{F_{CL,j}(\Delta x, t) - F_{CU}(\Delta x, t)}{2} \tag{9}$$

For what concerns the implementation of the code, The LTDPoliTO code has been developed in MATLAB, exploiting the arithmetic vector strategy that allows to obtain a high computational efficiency. The LTDPoliTO code is characterized by 4 stages:

- Loading of the input data from text files (slope and curve radius of the track, loading and unloading curves for coupling systems, driving cycle and the mechanical characteristics of traction motors and dynamic brake).

- Pre-processing stage for the definition of the train configuration and initial conditions, as well as for the re-interpolation of the input data characteristics using fixed discretization steps.
- Numerical solution of the differential equations by means of the variable step-size MATLAB ode solver ode15s[54, 55], which computes the position and speed of each vehicle for each time step.
- Post-processing stage: the deflections, the relative velocities and the in-train forces are obtained for each connection element in all time steps and they can be saved in binary files for further analysis or for storage purposes.

The re-interpolation of the input text files through fixed discretization steps in the pre-processing stage is the key to speed up the indexing operations for the calculation of the forces acting on each vehicle during the simulation, avoiding the use of loop flows that would slow down the computation. The variable step-size predictor-corrector stiff solver ode15s is also an efficient choice both for the accuracy of the results and the reduction of calculation times, since it auto-adjusts the time step during the simulation depending on whether the simulation error is within or above a tolerance range.

A further decrease in calculation times is obtained by passing to the solver the constant Jacobian sparsity pattern as an input, in order to reduce the number of elements in the Jacobian matrix to be calculated by the built-in routine for the Jacobian numerical estimation in the failed steps.

3. Simulation input data

In this section, the input data used for the simulations are presented. As mentioned before, data was taken from the International benchmark questions paper.[8]

For all simulations, the first train of the benchmark is considered, consisting of 2 leading locomotives and 50 wagons. Each locomotive has a total length of 22.95 m, including half of the coupling system on the front and on the rear, and 6 axles with an axle-load of 22.33 tonne, while the wagons comprise four axles with an axle-load of 32 tonne and have a total length of 15 m.

For the connection of the vehicles, the connection systems indicated by the benchmark, i.e., draw-bars and couplers, are used for the first two comparisons concerning the resistance laws, while in the last comparison concerning the connection element, the European buffer-hook system is used. The only difference between drawbars and couplers is the slack, which is 0 mm for the drawbars, 10 mm for the couplers, divided into 8 mm for the tensile state and 2 mm for the compressive state. The bars are used to form wagon pairs which are then connected by couplers. The locomotive-locomotive and locomotive-wagon connections are always performed through couplers. Figure 3a shows the mechanical force-deflection characteristic of the series of two draft gears and a coupler/bar both in tensile and compressive states, obtained from the benchmark data. In Figure 3a, also the mechanical characteristic of the buffer-hook system is plotted, obtained from the characteristic of a single buffer and a single hook considering that the two buffers on each side work in series, the two pairs instead work in parallel. The two hooks work in series, as in the case of the coupler. Please note from the detailed view of Figure 3a both the coupler slack and the

preload of the buffer-hook system. According to the benchmark rules, tensile forces and tensile deflections have a negative sign, the opposite for compressive state.

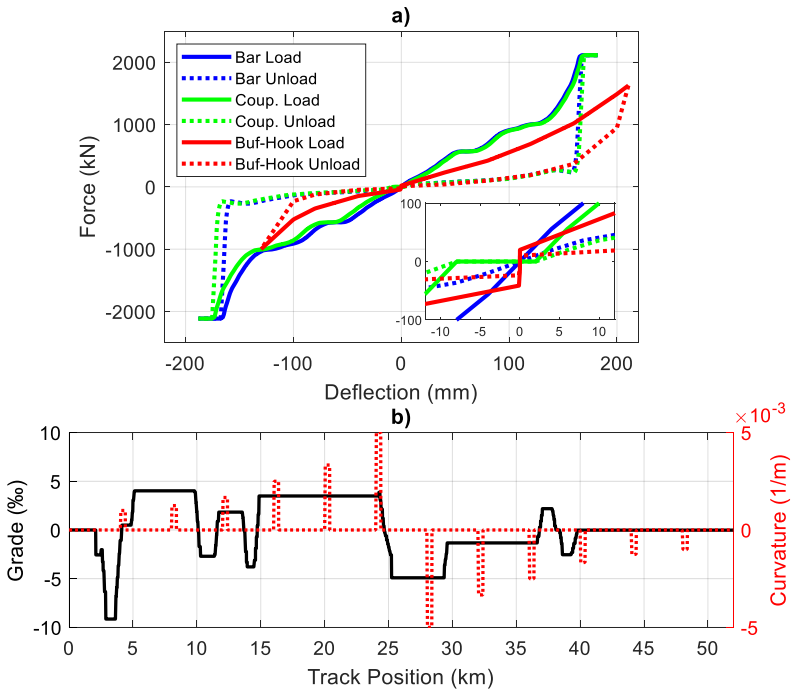

Figure 3: a) Force-deflection characteristics of coupler/bar and buffer-hook system. b) Track grade and curvature.

Locomotives have 8 notch levels for traction and dynamic braking, the conditions and the parameters used to generate traction and DB characteristics are specified in the benchmark questions paper. The leading locomotive driving cycle for each simulation scenario is given in the international benchmark as a function of the simulation time, and a 3 s shift is applied on the remote locomotives, i.e., the locomotives which are not directly connected to the leading locomotive, to represent the radio signal delay. However, the next section will show that for the sake of a fair comparison among different laws for the calculation of the resistant forces, the notch level should be defined as a function of the position of the leading locomotive.

The track has a length of 50 kilometers and is characterized by 12 curves, each one featuring a 50 m entry transition, a 300 m circular curve and a 50 m exit transition. Track curvatures and grades are again extracted from the benchmark input dataset and they are shown in Figure 3b, where positive values refer to uphill track sections and right-handed curves, while negative values are used for downhill track sections and left-handed curves.

In this paper the influence of the motion resistance laws and the coupling element on the simulation results are investigated, by performing three sets of simulations. More in detail, the first set of simulations is performed to assess the influence of the ordinary resistance law on the outputs results, using in the first simulation the benchmark law for both wagons and locomotives, in the second simulation the Russian law for all vehicles, in the third simulation two distinct Chinese laws for wagons and locomotives, and finally in the last one the benchmark law for wagons and the Chinese HXD2 law for locomotives. Please note that only the laws with the axle-load as an explicit parameter (benchmark and Russian law) and the two Chinese laws (China HXD2 loco and China full freight laws), which are valid for wagons with axle-load and wheel arrangement similar to those considered in the benchmark, are taken into account. The other expressions listed in Table 1, instead, are valid for vehicles with values of axle-load significantly different from the ones indicated in the benchmark, so they are not considered in this work.

In the second set of simulations, the influence of the curving resistance law is evaluated, while the ordinary resistant forces are calculated with the original expression suggested in the benchmark. The benchmark law, the Roeckl law and the wheelbase formula are compared. In the wheelbase formula, a is set equal to 2.032 meters for locomotives and to

1.95 meters for wagons, according to the typical values of the vehicles considered in the simulations.

Finally, the last set of simulations is performed to assess the influence of the coupling system. The first simulation in this set-is performed using the drawbars and couplers as suggested in the benchmark, while the second simulation is carried out by replacing the benchmark connection systems with buffer-hook systems. Of course, in this comparison, the expressions for the calculation of both propulsion and curving retarding forces are those suggested in the benchmark.

All the simulations performed are summarized in Table 2. Please note that simulation 1 for each simulation set is the reference simulation using all the expressions and input data provided by the benchmark.

Table 2: Comparison between different propulsion resistance laws.

1st set of simulations (Propulsion resistance)		
N. simulation	**Locomotive law**	**Wagon law**
Simulation 1	Benchmark (locomotive)	Benchmark (wagon)
Simulation 2	Russian	Russian
Simulation 3	China HXD2 loco	China full freight
Simulation 4	China HXD2 loco	Benchmark (wagon)
2nd set of simulations (Curving resistance)		
N. simulation	**Law**	
Simulation 1	Benchmark	
Simulation 2	Roeckl	
Simulation 3	Wheelbase formula	
3rd set of simulations (Coupling system)		
N. simulation	**Coupling system**	
Simulation 1	Coupler and bar	
Simulation 2	Buffer-hook system	

All simulations are performed by setting the relative tolerance and the absolute tolerance values to 1e-06 and 1e-07 respectively, the threshold value v_ε to 1e-3 m/s and adopting the following discretization steps for the input data:

• 0.01 mm for the coupling system deflections.

• 1 m for the track section length.

• 1 ms for the notch level characteristic.

• 1 mm/s for the locomotive speed.

4. Results

In this section, the results obtained from the three simulation sets are presented, focusing on the following outputs:

- Main outputs, as suggested in the benchmark results paper[9], namely, the maximum and average speed reached throughout the simulation among all vehicles, the largest in-train force for both tensile and compressive states among all the coupling systems, the mean value of the maximum tensile and compressive forces of all connecting systems and the maximum deflection registered on a selected coupling system position.
- The speed of the leading locomotive as a function of its position along the track.
- The ordinary and curving resistances of a selected vehicle as a function of its position (for the first and the second comparison).
- The in-train force on a specific coupling system as a function of the position of the first of the connected vehicles starting from the leading locomotive.
- The force-displacement (F-D) cross-plot of the selected coupling system.

According to the benchmark questions paper, the coupling system between the 10th and 11th vehicle is selected for the first two set of simulations. In the last set of simulations, the connection system between the 36th and 37th vehicles, on which traction forces are below the maximum value allowed for the European hook, is instead considered. Please note that in this section the benchmark vehicle numbering rule is adopted, which counts the vehicles in ascending order starting from the leading locomotive.

4.1 Modification of the driving control characteristic

In the original LTDPoliTO code, the driving control, i.e., the level of the notch regulated by the train driver, is given as a function of the simulation time, according to the benchmark prescription. In fact, the research group establishing the benchmark agreed that in this manner it would have been easier to deal with the implementation of the radio signal delay on the locomotives in the middle of the train composition, with no big discrepancies among the benchmark participants, since all simulators had to use the same expressions for the calculation of all the resistant forces. However, the authors of the benchmark questions paper specified that generally the driving control should be given as a function of the locomotive position.

The analyses carried out in this paper require the modification of the driving control characteristic, which must be provided as a function of the position of the leading locomotive. On the contrary, in fact, the simulation results would be affected by the different levels of notch at the same position of the leading locomotive in different simulations. In fact, due to the modification of the resistance laws or also of the vehicle connection systems, the leading locomotive could be in different track position in the various simulations, since the train speed depends on resistance laws and coupling system.

Consequently, if the notch level is given as a function of the simulation time, a different value is imposed to the locomotive at the same track position in different simulations, thus altering the comparison. This change is also justified from the physical point of view since the notch level mainly depends on the track characteristics and on the desired speed profile that the train driver wants to achieve. Therefore, the notch characteristic is reconstructed as a function of the position of the leading locomotive starting from the outputs computed by LTDPoliTO in the four benchmark simulation scenarios. The notch level applied to the leading locomotive is thus given as a function of its position, while in case a train configuration including remote locomotives was considered, the 3 s delay should be left unchanged, in accordance with the benchmark data, in order to simulate the radio communication delay. Obviously, this change has no effect on the first simulation of each comparison, that is the reference simulation using the benchmark input data. Please note that the 3 s delay is not applied in the simulations presented in the paper, which refer to the first benchmark simulation scenario, since the first train only has two locomotives at its head, directly connect to each other, and no remote locomotives are present in the train composition. Therefore, the same notch level is applied to both locomotives, as a function of the leading locomotive position along the track.

In Figure 4a, the leading locomotive notch level for the third simulation of the first comparison is shown in two different cases, i.e., i) when the notch is provided as a function of the simulation time and ii) when the notch characteristic is reconstructed as a function of the position of the leading locomotive. The two characteristics are significantly out of phase, consequently the comparison is completely altered, as can be seen for example in Figure 4 4b where the speed of the leading locomotive is shown for the four simulations, using the

notch characteristic as a function of the simulation time. In the following subsections, only the results obtained with the corrected notch characteristic, given as a function of the leading locomotive position, will be presented. Table 3 summarizes the main simulation outputs obtained from all the simulations performed in each of the three simulation sets, which will be discussed in the following subsections.

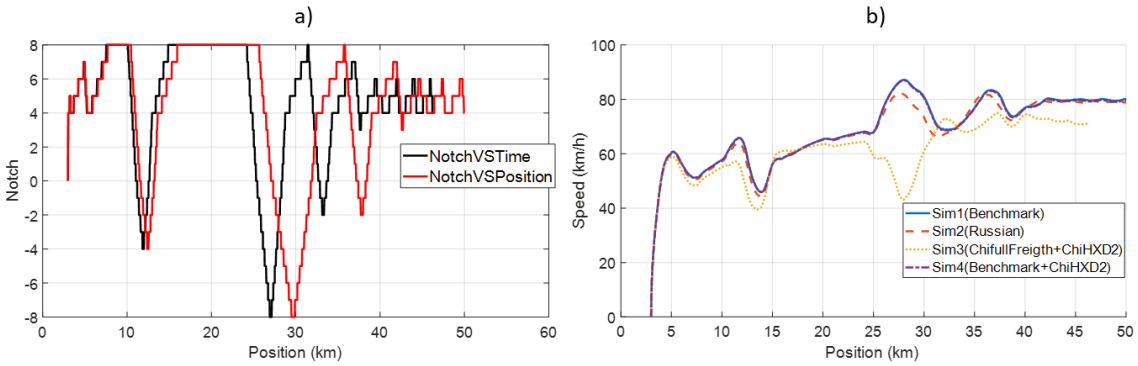

Figure 4: a) Level of notch of the leading locomotive in the third simulation (Chinese laws) if the notch is provided as a function of the time (black curve) or it is provided as a function of the position (red curve). b) Speed of the leading locomotive with the driving cycle given as a function of time.

Table 3: Main simulation outputs for all simulation sets.

			Largest in-train forces (kN) @coupler position		**Mean in-train forces (kN)**		**Max. deflection of selected coupler position (mm)**		
N. simulation	Max. speed (km/h)	Av. speed (km/h)	Tensile	Comp	Tensile	Comp	Pos	Tensile	Comp
First simulation set: Ordinary resistances									
1	87.31	65.43	-563@2	338@2	-336	194	10	-64.56	45.07
2	87.31	65.34	-563@2	338@2	-334	195	10	-64.77	45.03
3	81.67	58.48	-570@2	397@2	-340	214	10	-78.57	50.15
4	87.17	65.3	-564@2	340@2	-335	195	10	-64.53	45.3
Second simulation set: Curving resistances									
1	87.31	65.43	-563@2	338@2	-336	194	10	-64.56	45.07
2	87.31	65.34	-563@2	338@2	-334	195	10	-64.77	45.03
3	87.7	65.86	-563@2	339@2	-334	193	10	-64.19	44.74
Third simulation set: Coupling system									
1	87.31	65.43	-563@2	338@2	-336	194	36	-35.07	21.62

2	87.32	65.43	-564@2	339@2	-330	195	36	-60.11	34.04

4.2 Propulsion resistance comparison

From Table 3, considering the first simulation set, it can be noticed that the results of the second and fourth simulations agree with those obtained using the benchmark expression, both for speeds and in-train forces. On the other hand, the results of the third simulation, which uses two Chinese laws for wagons and locomotives, are significantly different, with a decrease of 6% and 10% in maximum and average speed respectively, and a remarkable increase in the in-train force and deflections of the selected coupling systems. In fact, the Chinese laws estimate a higher resistance than benchmark and Russian laws, as shown Figure 5a, where the propulsion resistance of the 10^{th} vehicle is represented. The values of resistant force predicted by the Chinese law for wagons are from 1.5 to 2 times higher than those computed with the Benchmark and Russian laws, at the same speed. This generates a decrease of the train speed, see Figure 5b, which is related to the difference in the resistant forces acting on the vehicles, however, due to the strong nonlinearity of the problem, the difference in the computed speed is not directly proportional to the difference in the computed resistant forces. Moreover, an increase of the in-train forces, both in traction and compression, can be observed in Figure 5c, which is related to the larger values of resistant forces computed with the laws from Chinese standards, too. Please note how the variation of the propulsion resistance law produces only a translation of the in-train force, since only the “static” component of the force is modified, whereas the “dynamic” one is not altered.

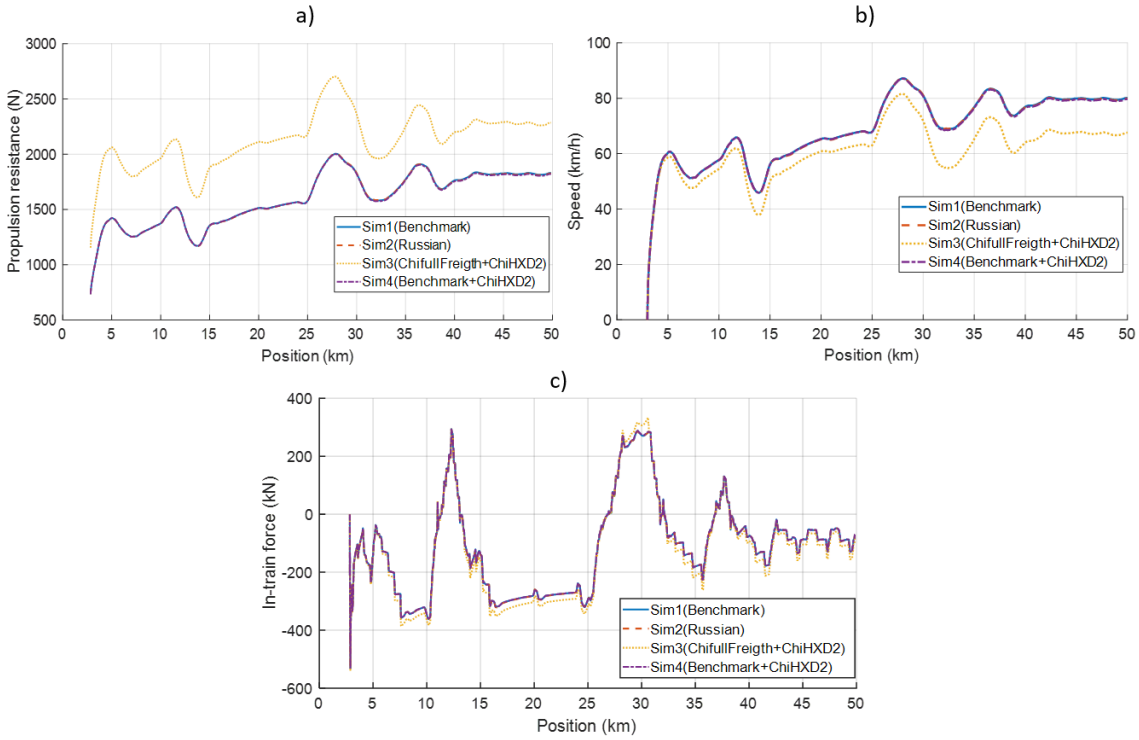

Figure 5: a) Propulsion resistance of the 10th vehicle. b) Speed of the leading locomotive. c) In-train force between 10th and 11th vehicles.

4.3 Curving resistance comparison

Focusing on the main outputs of the second simulation set shown in Table 3, they agree in terms of both in-train forces and velocities for all three curving resistance laws, with an increase of the values of maximum and average speed less than 1% in the third simulation (wheelbase formula). The wheelbase formula estimates lower values of curving resistance with respect to the other laws along all the track, while the highest resistance is given by the Roeckl formula, except for the curves at the 24th and 28th kilometers, where the benchmark formula estimates the highest resistant force, see Figure 6a. Figure 6b and Figure 6c show again the speed of the leading locomotive and the in-train force on the selected coupling system, respectively. In all three simulations, the results in terms of forces and speeds do not differ significantly, although slightly higher values of speed are calculated for the leading locomotive in case the wheelbase formula is used.

Of course, this consideration could be due to the low index of tortuosity of the track. Therefore, simulations not shown in the paper were carried out increasing the length of each curve in the track from 300 m to 600 m and 900 m. However, the results confirmed that the three laws for the calculation of the curving resistance lead to limited variations of the main simulation outputs.

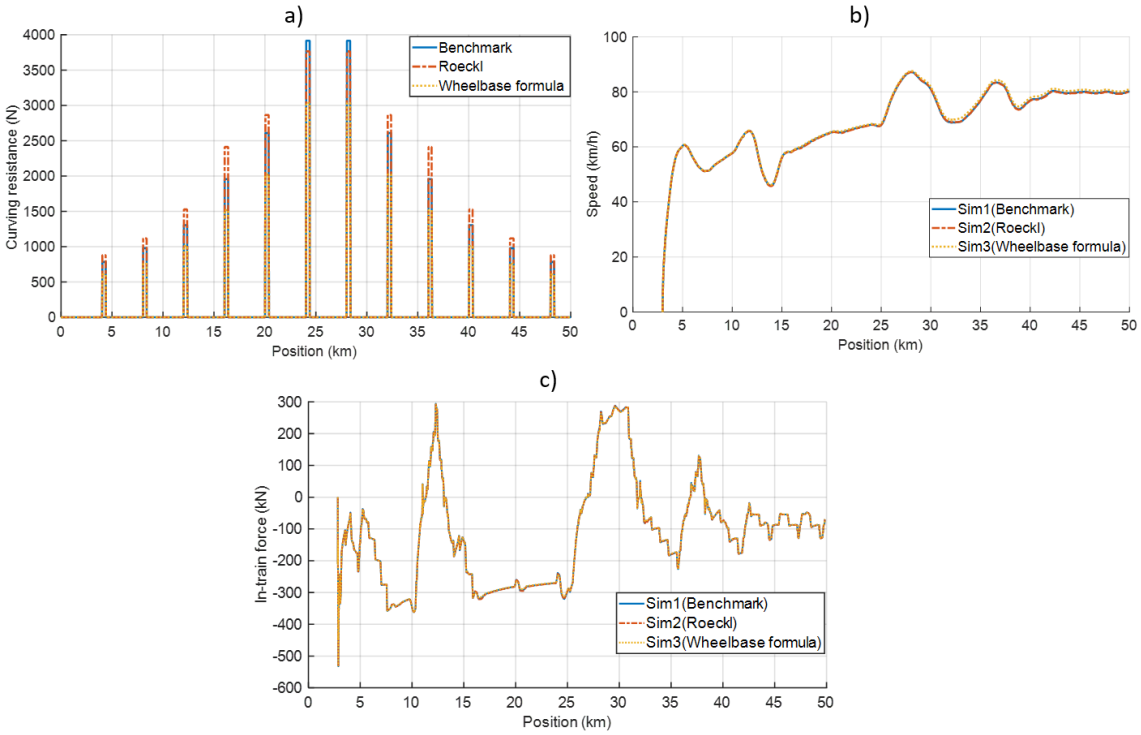

Figure 6: a) Curving resistance along the track. b) Speed of the leading locomotive. c) In-train force between 10th and 11th vehicles.

4.4 Coupling system comparison

From the main outputs of the third simulation set shown in Table 3, it can be noticed that the substitution of the coupler system with the European buffer-hook system does not significantly affect the values of maximum and average speed reached by the train and the values of in-train forces. On the other hand, the maximum deflections of the selected coupling system obtained with the European system are much higher than those obtained with couplers and bars, respectively of 57% and 71% for compression and tensile states. In

fact, the coupler/bar is much stiffer than the European coupling system, as it can be noticed in Figure 3a. Figure 7a shows the speed of the leading locomotives in the two simulations performed in this comparison, while Figure 7b and Figure 7c show the in-train forces and the deflections on the 36th connection system in the first train configuration of the international benchmark, on which the maximum tensile forces are below the limit value for the European hook (250 kN) throughout the simulation. Despite the values of in-train forces are not significantly different in the two simulations, the in-train force response obtained using the buffer-hook system shows a more vibrated pattern with greater amplitude and duration characterized by lower frequencies, see the detailed view of Figure 7b, since the European buffer-hook system is less stiff than the coupler or drawbar. Moreover, a cause for this vibration is also represented by the preloads of the buffer and of the hook, which are extremely difficult to manage numerically when a transition between tensile and compressive states occurs.

For both coupling systems, Figure 7c highlights the nonlinear transition paths of the in-train forces due to the transitions between the loading and unloading curves, which occurs when the relative speed on the coupling element is less than the threshold speed, set to 1e-3 m/s in all the simulations presented in this paper, see Equations 7-9. Figure 7d shows the maximum tensile and compressive forces of all couplers for the two simulations. The values of the in-train forces are below the maximum force supported by the buffer-hook system, according to the European standard EN 15566[56], although they are very close to the fatigue limits, especially in the vehicles close to the train head. Therefore, such load conditions would be excessively high in the long way

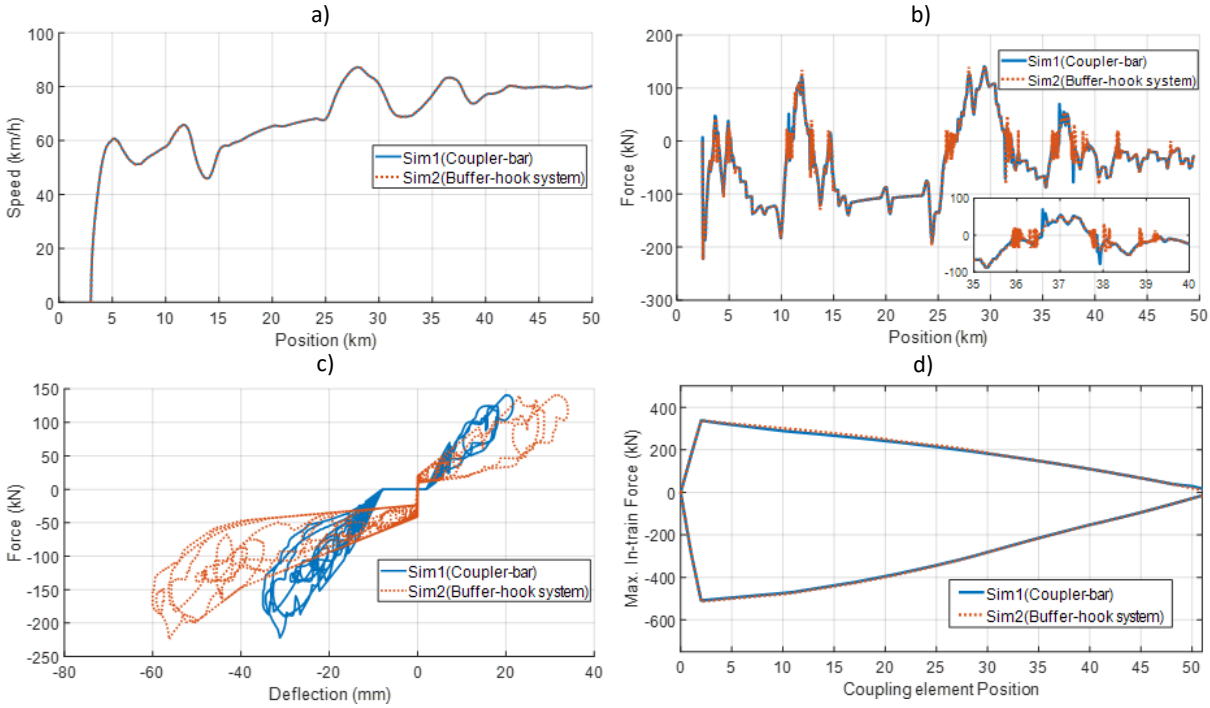

Figure 7: a) Speed of the leading locomotive. b) In-train force between 36th and 37th vehicles. c) Force - deflection cross plot of the 36th connection system. d) Maximum tensile and compressive forces on all coupling positions.

5. Conclusions

This paper deals with two fundamental topics of the longitudinal dynamic simulation of long freight trains, i.e., the modelling of the propulsion and curving resistance and the coupling system.

Simulations are performed on the first scenario of the International benchmark of LTD simulators, using the LTDPoliTO code. Compared to the code used for the benchmark simulations, it was necessary to modify the driving control, i.e., the notch level regulated by the train driver, expressing it as a function of the position of the leading locomotive instead of the simulation time, so that the differences between the simulations of each simulation set can only be related to the modification of the law of resistance or to the type of coupling system.

The first set of simulations, in which only the ordinary resistance law was changed from one simulation to another, showed that the modelling of propulsion resistances can have significant effects on the simulation outputs, both in terms of speed and in-train forces. It is therefore necessary to appropriately choose the propulsion resistance law, possibly using a law obtained on the specific vehicles under examination.

The second set of simulations, in which three different curving resistance laws were used, did not show instead significant differences. No big discrepancies arose even with an increase in length of the track curves, and this is probably related to the fact that with all the three laws considered, the curving resistance is lower than the ordinary resistances and than the resistant force due track grade.

Anyway, modifying the resistance laws produces only a translation of the in-train forces, since only the “static” component of the force is modified, whereas the “dynamic” one is not altered.

For what concerns the coupling system, the usage of the European hook-buffer system does not produce significant increases in the train speed and in the maximum coupling forces, while the deflections are much higher than those obtained with the coupler/bar, due to the different stiffness of the two systems. Nevertheless, the maximum forces on the coupler positions next to the train head are very close to the fatigue limits of the hook system. Therefore, for the future development of new European freight corridors, where longer trains could presumably be adopted, it will be necessary the use of the coupler system, since the European buffer-hook system can support significantly lower loads and shows excessive deflections if the loads are large.

Conflict of interests

On behalf of all authors, the corresponding author states that there is no conflict of interest.

References

1. Mickoski H, Mickoski I, Djidrov M and Zdraveski F. Mathematical model of new type of train buffer made of polymer absorber-Determination of dynamic impact curve for different temperatures. *Machines*. 2018; 6.
2. Garg VK and Dukkipati RV. *Dynamics of Railway Vehicle Systems*. Academic Press, 1984.
3. Zhang Z, Li G, Chu G, Zu H and Kennedy D. Compressed stability analysis of the coupler and buffer system of heavy-haul locomotives. *Vehicle System Dynamics*. 2015; 53: 833-55.
4. Cheli F, Di Gialleonardo E and Melzi S. Freight trains dynamics: effect of payload and braking power distribution on coupling forces. *Vehicle System Dynamics*. 2017; 55: 464-79.
5. Massa A, Stronati L, Aboubakr AK, Shabana AA and Bosso N. Numerical study of the noninertial systems: application to train coupler systems. *Nonlinear Dynamics*. 2012; 68: 215-33.
6. Auciello J. *Modellazione multibody di convogli ferroviari per lo studio della dinamica longitudinale*. PhD Thesis, Università degli Studi di Firenze, Italy, 2008.
7. Crescentini E. *Sviluppo di un codice di simulazione dinamica per lo studio di treni merci di futura generazione*. PhD Thesis, Università degli Studi di Roma "Tor Vergata", Italy, 2008.
8. Spiryagin M, Wu Q and Cole C. International benchmarking of longitudinal train dynamics simulators: benchmarking questions. *Vehicle System Dynamics*. 2017; 55: 450-63.
9. Wu Q, Spiryagin M, Cole C, et al. International benchmarking of longitudinal train dynamics simulators: results. *Vehicle System Dynamics*. 2018; 56: 343-65.
10. Cole C. Longitudinal Train Dynamics. *Handbook of Railway Vehicle Dynamics*. Boca Ratón: Taylor & Francis, 2006.
11. Cole C, Spiryagin M, Wu Q and Sun YQ. Modelling, simulation and applications of longitudinal train dynamics. *Vehicle System Dynamics*. 2017; 55: 1498-571.
12. Cole C. Improvements to wagon connection modelling for longitudinal train simulation. In: *Conference on railway engineering proceedings: engineering innovation for a competitive edge*, Rockhampton, Australia, 7-9 September 1998,
13. Wu Q, Cole C, Luo S and Spiryagin M. A review of dynamics modelling of friction draft gear. *Vehicle System Dynamics*. 2014; 52: 733-58.
14. Wu Q, Luo S, Qu T and Yang X. Comparisons of draft gear damping mechanisms. *Vehicle System Dynamics*. 2017; 55: 501-16.
15. Olshevskiy A, Olshevskiy A, Kim C-W and Yang H-I. An improved dynamic model of friction draft gear with a transitional characteristic accounting for housing deformation. *Vehicle System Dynamics*. 2018; 56: 1471-91.
16. Witt T and Müller L. Methods for the Validation of Algorithms for the Simulation of Longitudinal Dynamics. *Vehicle System Dynamics*. 1999; 33: 386-93.

17. Cantone L, Karbstein R, Müller L, Negretti D, Tione R and Geißler H. TrainDynamic simulation—a new approach. In: *8th world congress on railway research*, Seoul, Korea, 18-22 May 2008.
18. Cantone L. TrainDy: the new Union Internationale des Chemins de Fer software for freight train interoperability. *Proceedings of the Institution of Mechanical Engineers, Part F: Journal of Rail and Rapid Transit*. 2011; 225: 57-70.
19. Andersen DR, Mattoon D and Singh S. Train Operation and Energy Simulator (TOES) Validation-Part I: Unit Train Revenue Service. In: *ASME RTD*, October 1992.
20. Prabhakaran A, Trent R and Sharma V. *Impact performance of draft gears in 263,000 pound gross rail load and 286,000 pound gross rail load tank car service*. Report for Federal Railroad Administration. Report no. DOT/FRA/ORD-06/16, 2006.
21. Low E and Garg V. *Validation of Train Operations Simulator Computer Program*. Report for Association of American Railroads. Report no. AAR Rpt. R-335, 1978.
22. Wu Q, Luo S-h, Wei C and Ma W. Dynamics simulation models of coupler systems for freight locomotive. *Journal of Traffic and Transportation Engineering*. 2012; 12: 37-43.
23. Ward ED and Leonard RG. Automatic Parameter Identification Applied to a Railroad Car Dynamic Draft Gear Model. *Journal of Dynamic Systems, Measurement, and Control*. 1974; 96: 460-5.
24. Hsu T-K and Peters D. A simple dynamic model for simulating draft-gear behavior in rail-car impacts. *Journal of Engineering for Industry*. 1978; 100: 492-6.
25. Belforte P, Cheli F, Diana G and Melzi S. Numerical and experimental approach for the evaluation of severe longitudinal dynamics of heavy freight trains. *Vehicle System Dynamics*. 2008; 46: 937-55.
26. Cheli F and Melzi S. Experimental Characterization and Modelling of a Side Buffer for Freight Trains. *Proceedings of the Institution of Mechanical Engineers, Part F: Journal of Rail and Rapid Transit*. 2010; 224: 535-46.
27. Cruceanu C, Spiroiu M, Craciun C, Tudorache C and Dumitriu M. Aspects concerning the longitudinal dynamics of passenger trains during braking actions. In: *3rd WSEAS international conference on applied and theoretical mechanics*, Puerto De La Cruz, Tenerife, Canary Islands, Spain, 14-16 December 2007, pp. 14-6.
28. Cruceanu C, Oprea R, Spiroiu M, Craciun C and Arsene S. Computer aided study regarding the influence of filling characteristics on the longitudinal reactions within the body of a braked train. In: *13th WSEAS International Conference on COMPUTERS*, Rhodes, Greece, 22-25 July 2009, WSEAS.
29. Craciun C, Mitu A, Cruceanu C and Siretanu T. Modeling the buffers hysteretic behavior for evaluation of longitudinal dynamic in-train forces. In: *The annual symposium of the institute of solid mechanics, SISOM 2012 and session of the commission of acoustics*, Bucharest, 30-31 May 2012.
30. Oprea RA. Longitudinal dynamics of trains—a non-smooth approach. *Nonlinear Dynamics*. 2012; 70: 1095-106.
31. Oprea RA, Cruceanu C and Spiroiu MA. Alternative friction models for braking train dynamics. *Vehicle System Dynamics*. 2013; 51: 460-80.
32. Oprea RA. A constrained motion perspective of railway vehicles collision. *Multibody System Dynamics*. 2013; 30: 101-16.

33. Wu Q, Spiryagin M and Cole C. Longitudinal train dynamics: an overview. *Vehicle System Dynamics*. 2016; 54: 1688-714.
34. Chang C, Guo G, Wang J and Ma Y. Study on longitudinal force simulation of heavy-haul train. *Vehicle System Dynamics*. 2017; 55: 571-82.
35. Wu Q, Spiryagin M and Cole C. A dynamic model of friction draft gear In: *Proceedings of the ASME Design Engineering Technical Conference*, Buffalo, New York, 17-20 August 2014.
36. Wu Q, Spiryagin M and Cole C. Advanced dynamic modelling for friction draft gears. *Vehicle System Dynamics*. 2015; 53: 475-92.
37. Rochard BP and Schmid F. A review of methods to measure and calculate train resistances. *Proceedings of the Institution of Mechanical Engineers, Part F: Journal of Rail and Rapid Transit*. 2000; 214: 185-99.
38. Boschetti G and Mariscotti A. The parameters of motion mechanical equations as a source of uncertainty for traction systems simulation. In: *20th IMEKO World Congress*, Busan, Korea, 9-14 September 2012, pp. 897-902.
39. Locomotive and Train Resistance: 5AT Advanced steam locomotive project. https ://5at.co.uk/index.php/definitions/terrms-and-definitions/resistance.html (2012, accessed 05 November 2020)
40. Radosavljevic A. Measurement of train traction characteristics. *Proceedings of the Institution of Mechanical Engineers, Part F: Journal of Rail and Rapid Transit*. 2006; 220: 283-91.
41. Maksym Spiryagin, Colin Cole, Yan Quan Sun, Mitchell McClanachan, Valentyn Spiryagin and McSweeney T. Longitudinal Train Dynamics. *Design and Simulation of Rail Vehicles*. Boca Raton: CRC Press, 2014.
42. Muller AE. Starting diagram of electric trains with motors having a series characteristxc. *THE BROWN BOVERI REVIEW*. 1923; 10: 108-15.
43. Sachs K. Triebfahrzeuge für Gleichstrom. *Elektrische Triebfahrzeuge*. Springer, 1973, p. 1134-399.
44. Polach O. A Fast Wheel-Rail Forces Calculation Computer Code. *Vehicle System Dynamics*. 1999; 33: 728-39.
45. Bosso N, Soma A and Gugliotta A. Introduction of a wheel-rail and wheel-roller contact model for independent wheels in a multibody code. In: *ASME/IEEE Joint Railroad Conference*, Washington, DC, USA, 23-25 April 2002, pp. 151-9.
46. Polach O. Creep forces in simulations of traction vehicles running on adhesion limit. *Wear*. 2005; 258: 992-1000.
47. Bosso N, Gugliotta A and Zampieri N. RTCONTACT: An Efficient Wheel-Rail Contact Algorithm for Real-Time Dynamic Simulations. In: *2012 Joint Rail Conference*, Philadelphia, Pa, 17-19 April 2012, pp. 195-204. New York: ASME.
48. Bosso N and Zampieri N. A Novel Analytical Method to Calculate Wheel-Rail Tangential Forces and Validation on a Scaled Roller-Rig. *Advances in Tribology*. 2018.
49. Bosso N, Magelli M and Zampieri N. Development and validation of a new code for longitudinal train dynamics simulation. *Proceedings of the Institution of Mechanical Engineers, Part F: Journal of Rail and Rapid Transit*. 2020.
50. Bosso N, Magelli M and Zampieri N. Long Train Dynamic Simulation by means of a New In-House Code. In: *WIT Transactions on The Built Environment*, 2020.

51. Bosso N, Magelli M and Zampieri N. Validation of a New LTD Code for Time Domain Simulations and Modal Analyses *Submitted to International Journal of Transport Development and Integration*. 2021.
52. Bosso N and Zampieri N. Long train simulation using a multibody code. *Vehicle System Dynamics*. 2017; 55: 552-70.
53. Bosso N, Gugliotta A and Zampieri N. A Mixed Numerical Approach to Evaluate the Dynamic Behavior of Long Trains. *Procedia Structural Integrity*. 2018; 12: 330-43.
54. Shampine LF and Reichelt MW. The MATLAB ode suite. *SIAM Journal of Scientific Computing*. 1997; 18: 1-22.
55. Shampine LF, Gladwell I, Shampine L and Thompson S. *Solving ODEs with matlab*. Cambridge university press, 2003.
56. EN 15566: 2016. Railway applications —Railway rolling stock — Drawgear and screw coupling.